Supporting Information

(*Z*)-Tetraphenylbut-2-ene-1,4-diones: Facile Synthesis, Tunable Aggregation-Induced Emission and Fluorescence Acid Sensing

Mengwei Li,[1,2] Yi-Xuan Wang,[1,2] Jianhui Wang,*[,1] and Yulan Chen*[,1]

1. Tianjin Key Laboratory of Molecular Optoelectronic Science, Department of Chemistry, Tianjin University, Tianjin, 300354, P. R. China

2. The authors contributed equally to this work

*E-mail: yulan.chen@tju.edu.cn; wjh@tju.edu.cn

Phone/Fax: +86-22-27404118

Experimental Section.

General. Unless noted otherwise, all chemicals were purchased from Aldrich, Acros or Adamas and used without further purification. Dichloromethane (DCM) and tetrahydrofuran (THF) were dried by usual methods before use. All reactions were performed under an atmosphere of nitrogen and monitored by TLC. Column chromatography was carried out on silica gel (200–300 mesh).

Measurements. ^{1}H NMR (400 MHz) and ^{13}C NMR (100 MHz) spectra were recorded on a 400 MHz Bruker AV 400 spectrometer. Matrix assisted laser desorption ionization time-of-flight mass spectroscopy (MALDI-TOF) was performed on a miorOTOF-QII mass spectrometer (Bruker Daltonics) using α-cyano-4-hydroxycinnamic acid as the matrix. UV-Vis absorption spectra were obtained on a PerkinElmer Lambda 750 UV/VIS/NIR spectrometer. Fluorescence and delayed PL emission spectra were recorded on a Hitachi F-7000 fluorescence spectrophotometer. The transient fluorescence decay curves and quantum yields of solid powders were measured on an Edinburgh FLS 920 fluorescence spectrometer. The powder X-ray diffraction patterns were recorded by Rigaku D/MAX-2500 X-ray diffractometer with Cu Kα radiation (λ = 1.5418 Å) (scan range: 5–40°). Particle size distribution of aggregates were measured on a Brookhaven ZetaPALS zeta potential analyzer. Geometric structures of

molecules were studied theoretically in the gas phase. Density functional theory (DFT) calculations were performed in Gaussian 09 software at the B3LYP functional with the 6-31G* basis set level.

Preparation of Aggregates.[S1] Stock solutions (1 mM) of AIE-active molecules in THF were prepared. An aliquot (0.1 mL) of the stock solution was diluted with an appropriate amount of THF in a volumetric flask (5 mL), and then water was added dropwise under vigorous stirring. A series of THF/water solutions were obtained with different water fractions (f_w) ranging from 0 to 95 vol%.

The fluorescence response of **TPBD-1** to acid vapor was measured according to the following steps:[S2] (1) Appropriate amount of acids was injected into a bottle (200 mL), and then saturated vapors were achieved after sealed at room temperature overnight. (2) Filter papers (1 cm × 1 cm) were immersed into the chloroform solution of **TPBD-1** (1 mM) for 10 min, removed and dried at 80 ^{o}C for 2 h. (3) Another bottle (10 mL) with filter paper inside was vacuumed, and saturated acid vapor (10 mL) was injected. The paper was exposed to the saturated vapors of different acids for 5 min. (4) Fluorescence spectra were measured immediately after the filter paper removed from the sealed bottle.

Synthesis:

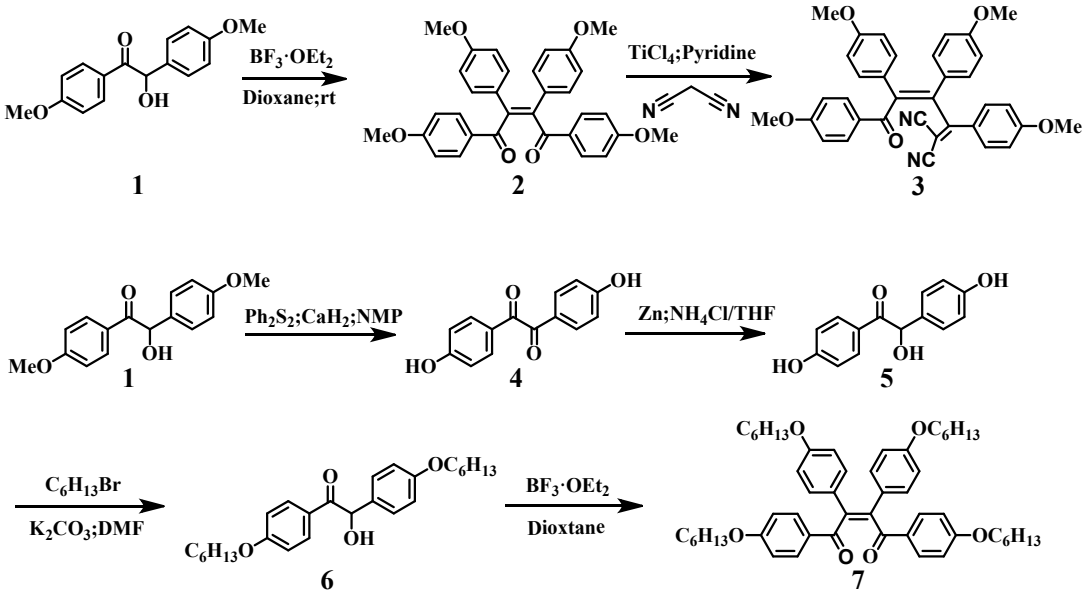

(*Z*)-1,2,3,4-Tetrakis(4-methoxyphenyl)but-2-ene-1,4-dione (2). To a stirred solution of 4,4'-dimethoxybenzoin **1** (10 mmol, 2.72 g) in 1,4-dioxane (10 mL), $BF_3{\cdot}OEt_2$ (60 mmol, 7.6 mL) was added gradually at room temperature, and stirred overnight. The reaction mixture was then poured into saturated $NaHCO_3$ solution to decompose the $BF_3{\cdot}OEt_2$ complex and extracted with diethyl ether. The combined organic extracts were dried over anhydrous $MgSO_4$, filtered and concentrated under vacuum. The residue was purified by column chromatography eluting with petroleum ether/ethyl acetate (10:1, v/v) to afford **2** as a yellow solid (1.57 g, 60%). ^1H NMR ($CDC1_3$, 400 MHz): δ 7.82 (d, 4H, ArH), 7.10 (d, 4H, ArH), 6.79 (d, 4H, ArH), 6.72 (d, 4H, ArH), 3.79 (s, 6H, CH_3), 3.74 (s, 6H, CH_3). ^{13}C NMR ($CDCl_3$, 100 MHz): δ 195.9, 163.3, 159.3, 142.4, 132.5, 131.1, 129.7, 128.1, 114.1, 113.5, 55.4, 55.1. m.p., 186–186.8 ^oC. MALDI-TOF (m/z), calculated for $C_{32}H_{28}O_6$ $[M + Na]^+$, 531.1778; found, 531.1778.

(*Z*)-2-(1,2,3,4-Tetrakis(4-methoxyphenyl)-4-oxobut-2-en-1-ylidene)malononitrile (3). In a two-necked flask, **2** (1.01 g, 2 mmol) and malononitrile (660 mg, 10 mmol) were dissolved in 20 mL 1,2-dichloroethane. The mixture was cooled to 5 ^{o}C (ice/water bath) under N_2, and titanium tetrachloride (1.6 mL, 15 mmol) and pyridine (3.2 mL, 20 mmol) were added dropwise over 60 min, successively. The solution was then heated to reflux overnight. After cooled to room temperature, the reaction mixture was filtered through celite and washed with chloroform. The filtrate was washed with 10% HCl (aq) and 10% $NaHCO_3$ (aq). The organic phase was combined, dried over $MgSO_4$ and concentrated. The residue was purified by column chromatography eluting with petroleum ether/ethyl acetate (10:1, v/v) to afford **3** as a red solid (400 mg, 36%). ^{1}H NMR ($CDC1_3$, 400 MHz): δ 7.83 (d, 2H, ArH), 7.76 (d, 2H, ArH), 7.08 (d, 2H, ArH), 7.02 (d, 2H, ArH), 6.86 (d, 2H, ArH), 6.79 (d, 2H, ArH), 6.71 (t, 4H, ArH), 3.80 (d, 6H, CH_3), 3.75 (d, 6H, CH_3). ^{13}C NMR ($CDCl_3$, 100 MHz): δ 194.3, 175.4, 163.6, 163.3, 159.7, 145.9, 139.2, 133.2, 131.6, 131.5, 128.9, 128.6, 128.4, 126.1, 114.5, 114.3, 114.2, 114.2, 114.0, 113.6, 80.6, 55.5, 55.4, 55.2, 55.2. MALDI-TOF (m/z), calculated for $C_{35}H_{28}N_2O_5$ $[M\bullet]^+$, 556.1998; found, 556.2038.

4,4'-Dihydroxybenzil (4). 4,4'-dimethoxybenzoin **1** (272 mg, 1 mmol) in 1-methyl-2-pyrrolidinone (0.8 mL) was added to a magnetically stirred mixture of Ph_2S_2 (260 mg, 1.2 mmol) and CaH_2 (140 mg, 3.2 mmol) in

NMP (1.2 mL) under N_2. The mixture was heated under reflux for 30 min. After cooled to room temperature, the reaction mixture was extracted with Et_2O (3 × 10 mL) to separate any neutral component. The combined organic extracts were washed with 5% aqueous NaOH (10 mL). The aqueous portion was collected and acidified in an ice bath with 6 M HCl and extracted with diethyl ether (3 × 15 mL). The combined organic phase was dried over anhydrous $MgSO_4$, filtered and concentrated under vacuum. The residue was then purified by column chromatography eluting with petroleum ether/diethyl ether (5:1, v/v) to afford **4** as a pale yellow solid (207 mg, 85%). ^{1}H NMR (DMSO-d_6, 400 MHz): δ 10.84 (s, 2H), 7.74 (d, 4H), 6.93 (d, 4H). ^{13}C NMR (DMSO-d_6, 100 MHz): δ 194.2, 164.4, 132.7, 124.7, 116.6.

4,4'-Dihydroxybenzoin (5). Zinc dust (780 mg, 12 mmol) was added to a vigorously stirred solution of 4,4'-dihydroxybenzil (484 mg, 2 mmol) which was dissolved in a mixture solution of saturated aqueous NH_4Cl and THF (1:1, v/v). The solution was stirred at room temperature overnight. After that, zinc-dust residue was filtered, filtrates were extracted with diethyl ether (3 × 5 mL), dried over anhydrous $MgSO_4$, filtered and concentrated under vacuum, which was then purified by recrystallized in petroleum ether/diethyl ether to obtain the product **5** as a white solid (411 mg, 85%). m.p., 181.8–182.7 ^{o}C. ^{1}H NMR (DMSO-d_6, 400 MHz): δ 10.38 (s, 1H, OH), 9.41 (s, 1H, OH), 7.88 (d, 2H, ArH), 7.19 (d, 2H, ArH), 6.78

(d, 2H, ArH), 6.68 (d, 2H, ArH), 5.88 (d, 1H, CH), 5.58 (d, 1H, OH). ^{13}C NMR (DMSO-d_6, 100 MHz): δ 197.9, 162.5, 157.3, 131.9, 131.2, 129.0, 126.4, 115.6, 115.6, 75.1.

4,4'-Dihexyloxybenzoin (6). A mixture of 4,4-dihydroxybenzoin (244 mg, 1 mmol), 1-bromohexane (396 mg, 2.4 mmol) and potassium carbonate (828 mg, 6 mol) in DMF (5 mL) was stirred at 80 ^{o}C overnight. The reaction mixtures were poured into water and extracted with diethyl ether. The organic phase was dried over anhydrous $MgSO_4$, filtered and concentrated under vacuum. The residue was then purified by column chromatography eluting with petroleum ether/diethyl ether (10:1, v/v) to afford **6** as a white solid (329 mg, 80%).[S3] m.p., 40.4–41.2 ^{o}C. ^{1}H NMR ($CDC1_3$, 400 MHz): δ 7.88 (d, 2H, ArH), 7.23 (d, 1H, ArH), 6.83 (dd, 4H, ArH), 5.84 (d, 1H, CH), 4.58 (d, 1H, OH), 3.96 (t, 2H, CH_2), 3.89 (t, 2H, CH_2), 1.75 (m, 4H, CH_2), 1.42 (m, 4H, CH_2), 1.32 (m, 8H, CH_2), 0.89 (m, 6H, CH_3). ^{13}C NMR ($CDCl_3$, 100 MHz): δ 197.3, 163.6, 159.2, 131.7, 131.6, 129.0, 126.1, 115.0, 114.3, 75.3, 68.3, 68.0, 31.6, 31.5, 29.2, 29.0, 25.7, 25.6, 22.6, 22.6, 14.0, 14.0.

(*Z*)-1,2,3,4-Tetrakis(4-(hexyloxy)phenyl)but-2-ene-1,4-dione (7). To a stirred solution of **6** (2 mmol, 824 mg) in 1,4-dioxane (10 mL), $BF_3{\cdot}OEt_2$ (12 mmol, 1.5 mL) was added gradually at room temperature and stirred overnight. The reaction mixtures were then poured into saturated $NaHCO_3$ solution to decompose the $BF_3{\bullet}$ OEt_2 complex and extracted with diethyl

ether. The combined organic extracts were dried over anhydrous $MgSO_4$, filtered and concentrated under vacuum. The residue was purified by column chromatography eluting with petroleum ether/ethyl acetate (10:1, v/v) to afford **7** as a yellow oil (473 mg, 60%). ^{1}H NMR ($CDC1_3$, 400 MHz): δ 7.81 (d, 4H, ArH), 7.09 (d, 4H, ArH), 6.77 (d, 4H, ArH), 6.70 (d, 4H, ArH), 3.92 (t, 4H, CH_2), 3.87 (t, 4H, CH_2), 1.73 (m, 8H, CH_2), 1.41 (m, 8H, CH_2), 1.31 (m, 16H, CH_2), 0.89 (t, 12H, CH_3). ^{13}C NMR (100 MHz, $CDCl_3$): δ 196.0, 162.9, 158.9, 142.3, 132.5, 131.1, 129.5, 128.0, 114.6, 114.0, 68.1, 67.9, 31.6, 31.5, 29.2, 29.0, 25.7, 25.7, 22.6, 14.0. MALDI-TOF (m/z): calculated for $C_{52}H_{68}O_6$ $[M + Na]^+$, 811.4908; found, 811.4909.

Supporting Figures:

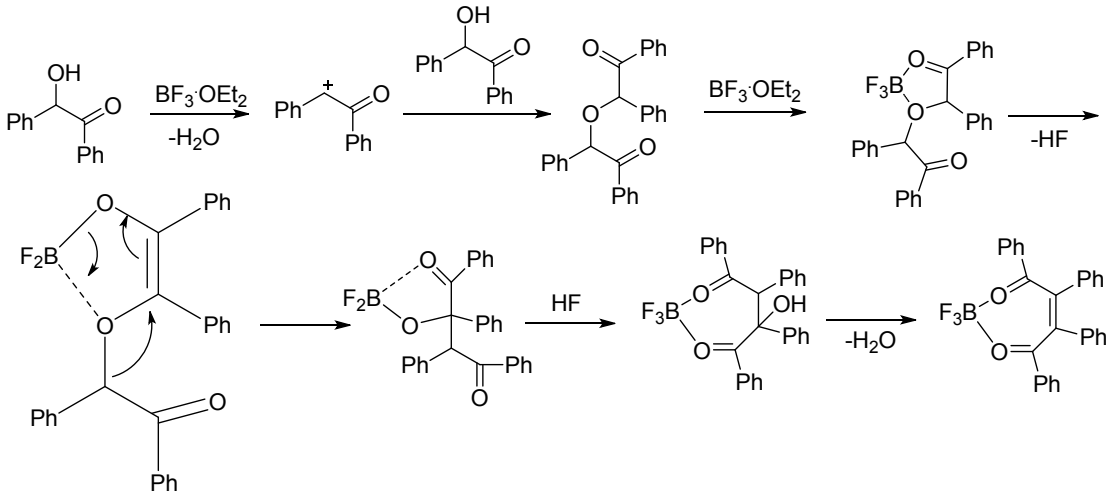

Scheme S1. Proposed mechanism for the formation of (*Z*)-tetraphenylbut-2-ene-1,4-dione.

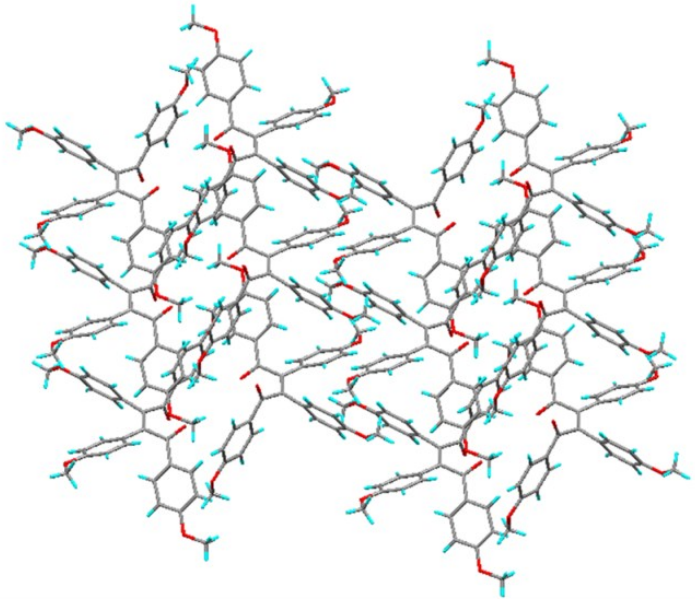

Figure S1. Stacking mode of **TPBD-1** in single crystal state.

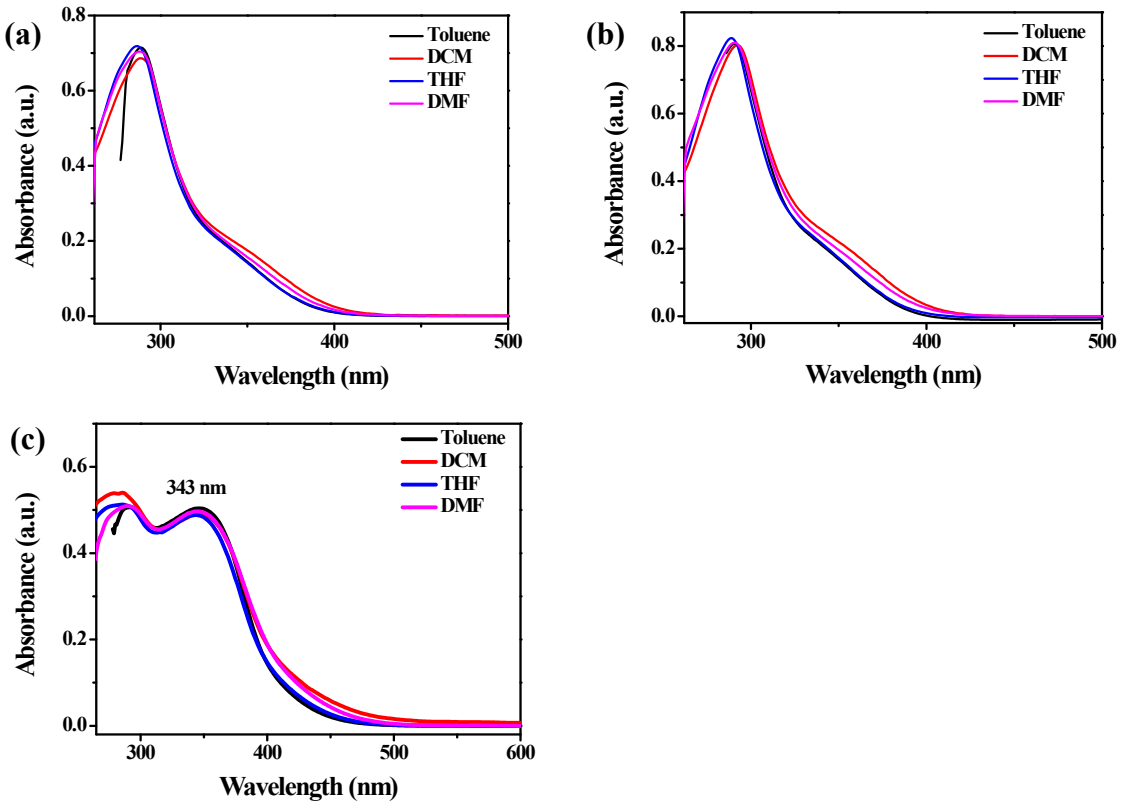

Figure S2. UV-Vis absorption spectra of (a) **TPBD-1**, (b) **TPBD-2**, and (c) **TPBD-CN** in different solvents (concentration: 2×10^{-5} M).

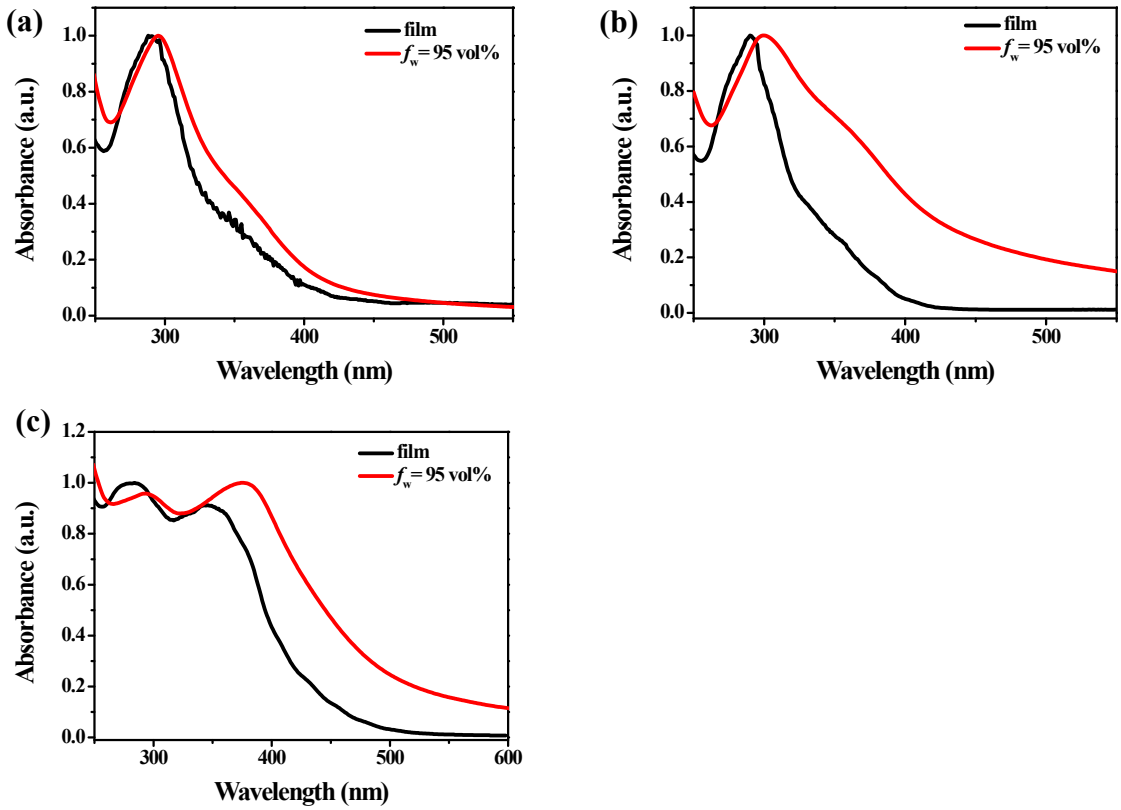

Figure S3. UV-Vis absorption spectra of (a) **TPBD-1**, (b) **TPBD-2**, and (c) **TPBD-CN**

in the film state (black line) and THF/water mixtures (f_w = 95 vol%, concentration: 2 × 10^{-5} M, red line).

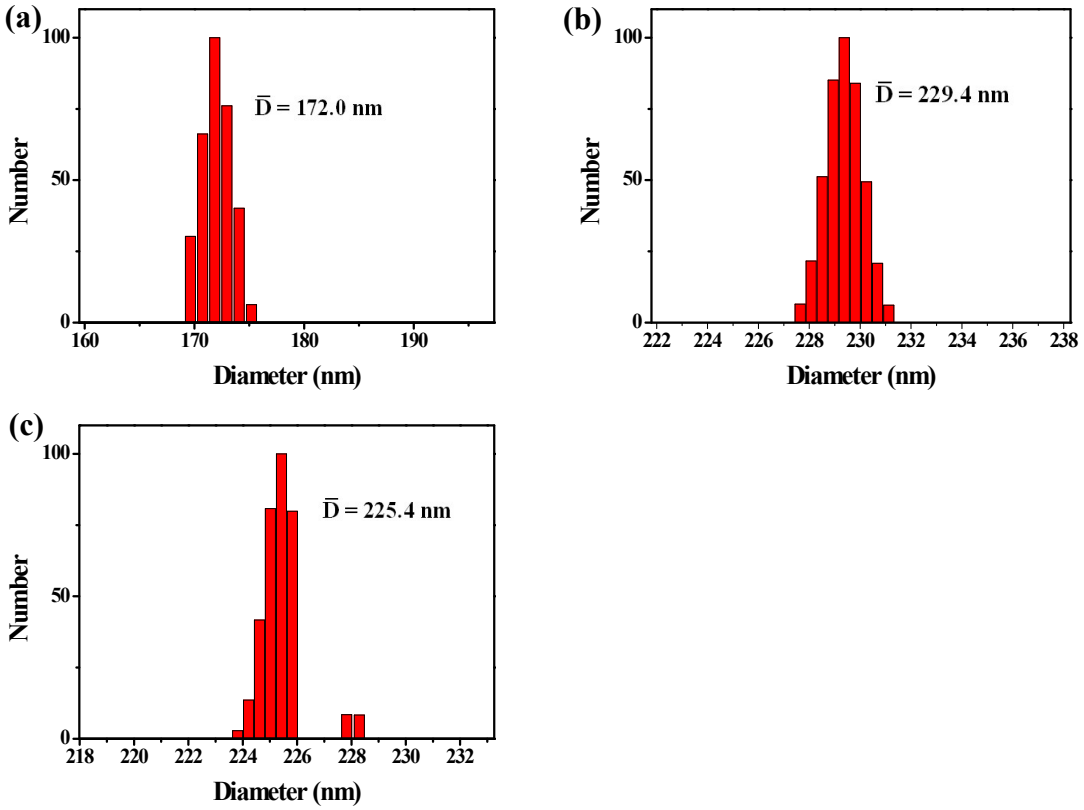

Figure S4. Hydrodynamic radius distribution of (a) **TPBD-1**, (b) **TPBD-2**, and (c) **TPBD-CN** in THF/water mixtures (f_w = 95 vol%, concentration: 2 × 10^{-5} M).

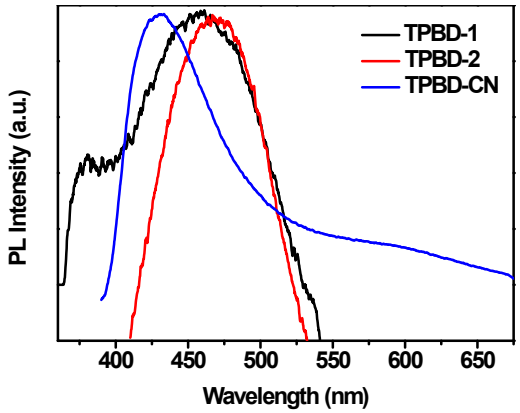

Figure S5. Fluorescence spectra of **TPBD-1**, **TPBD-2** and **TPBD-CN** in THF measured by signal amplification (concentration: 2 × 10^{-5} M; excitation wavelength for **TPBD-1**: 290 nm; for **TPBD-2**: 287 nm, and for **TPBD-CN**: 355 nm).

Table S1. Photophysical properties of **TPBD-1**, **TPBD-2** and **TPBD-CN**

	Solution[a,b]		Aggregate[a,c]		Solid[d]	
Samples	λ_{em} (nm)	Φ_F	λ_{em} (nm)	Φ_F	λ_{em} (nm)	Φ_F
TPBD-1	460	0.06%	500	2.53%	460	2.33%
TPBD-2	470	0.09%	490	0.37%	--	--
TPBD-CN	430, 600 (sh)[e]	0.05%	585	5.25%	602	25.18%

[a]Measured using quinine sulphate in 0.1 M H_2SO_4 as standard (0.54); [b]Measured in THF; [c]Aggregates formed in THF/water mixtures with f_w = 95 vol%; [d]Determined by absolute method; [e]sh: shoulder peak.

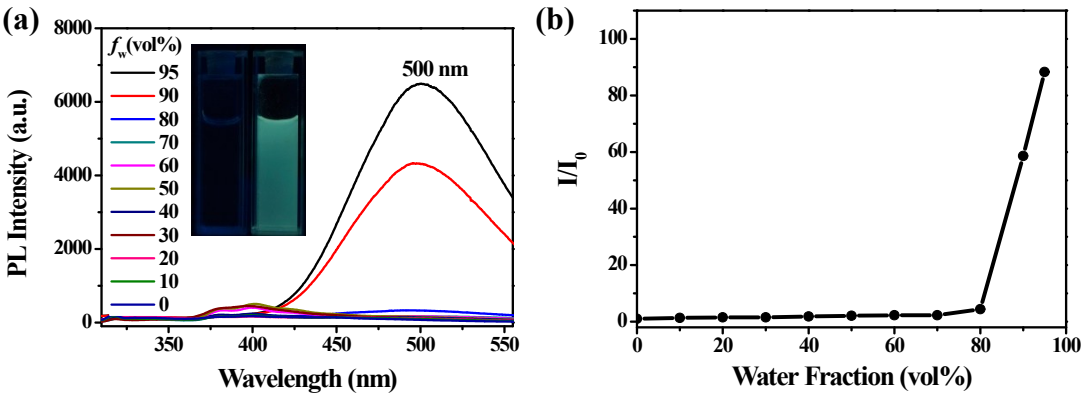

Figure S6. (a) Fluorescence spectra of **TPBD-1** in THF/water mixtures with different water fractions f_w (concentration: 2×10^{-5} M; excitation wavelength: 290 nm); (b) Plot of relative PL intensity (I/I_0) *vs* f_w. Inset: Photographs of **TPBD-1** in THF (left) and THF/water mixtures (f_w = 90 vol%, right) under the illumination with 365 nm UV light.

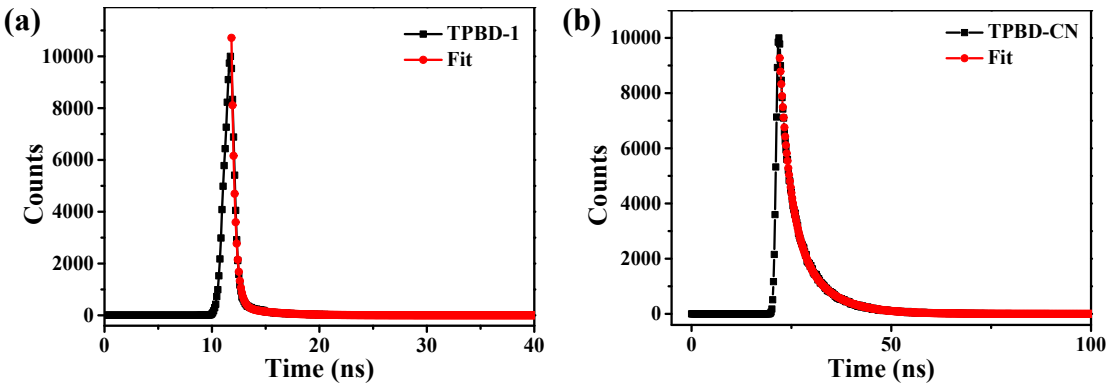

Figure S7. Fluorescence decay curve (black line) of (a) **TPBD-1** and (b) **TPBD-CN** in solid state. Red line: fitting of the fluorescence decay curve.

Table S2. Fluorescence decay of **TPBD-1** and **TPBD-CN** in solid state

		Fluorescence decay			
Samples	A_1/A_2[a]	τ_1 (ns)	τ_2 (ns)	χ^2	$\langle\tau\rangle$ (ns)[b]
TPBD-1	79/21	0.34	3.00	1.023	0.90
TPBD-CN	34/66	2.61	7.82	1.008	6.04

[a]Fraction (A, %) and lifetime (τ, ns) of (1) shorter or (2) longer lived species. [b]The mean lifetime $\langle\tau\rangle$ was calculated according to $\langle\tau\rangle = (A_1\tau_1 + A_2\tau_2)/(A_1 + A_2)$.

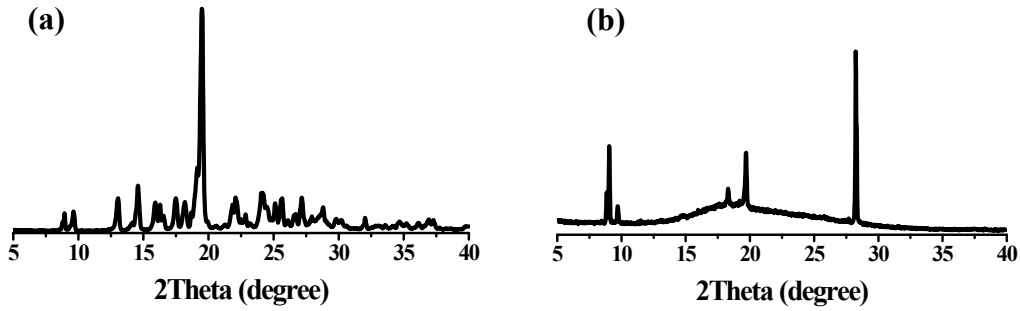

Figure S8. XRD spectra of **TPBD-1** in (a) crystal phase and (b) film state.

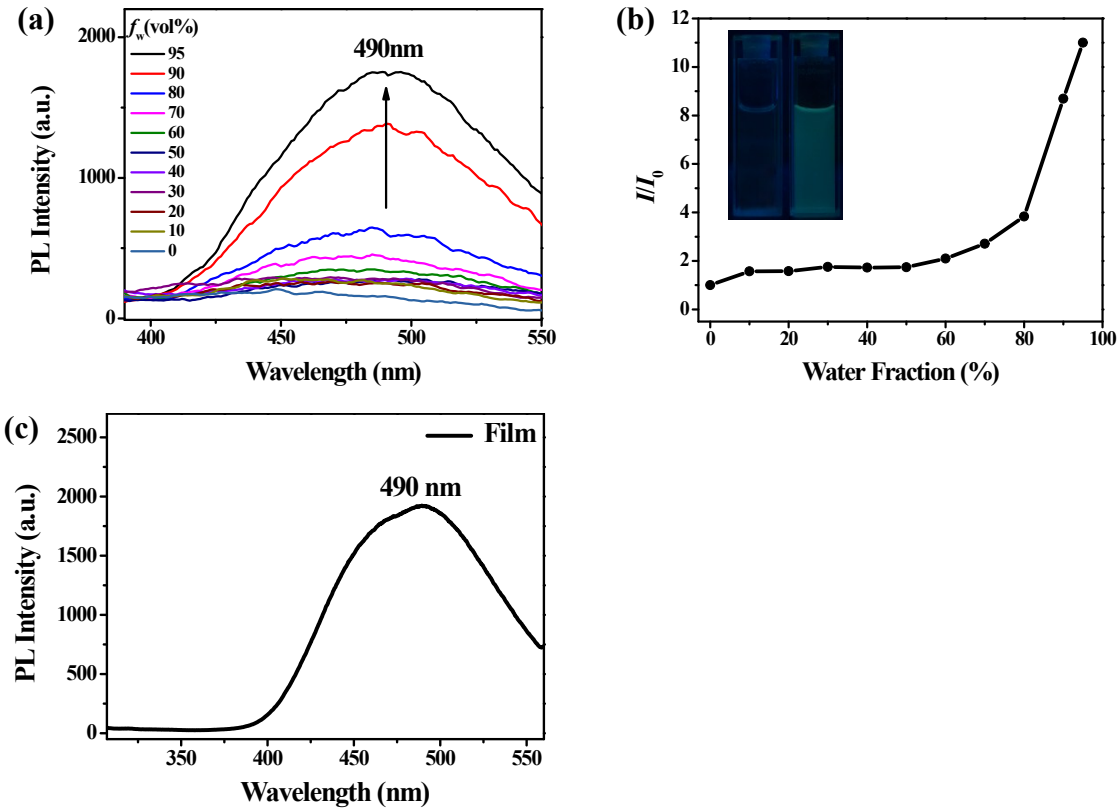

Figure S9. (a) Fluorescence spectra of **TPBD-2** in THF/water mixtures with different water fractions f_w (concentration: 2×10^{-5} M); (b) Plot of relative PL intensity (I/I_0) *vs* f_w; (c) Fluorescence spectrum of **TPBD-2** in film (excitation wavelength: 287 nm). Inset: Photographs of **TPBD-2** in THF (left) and THF/water mixtures (f_w = 90 vol%, right) under the illumination with 365 nm UV light.

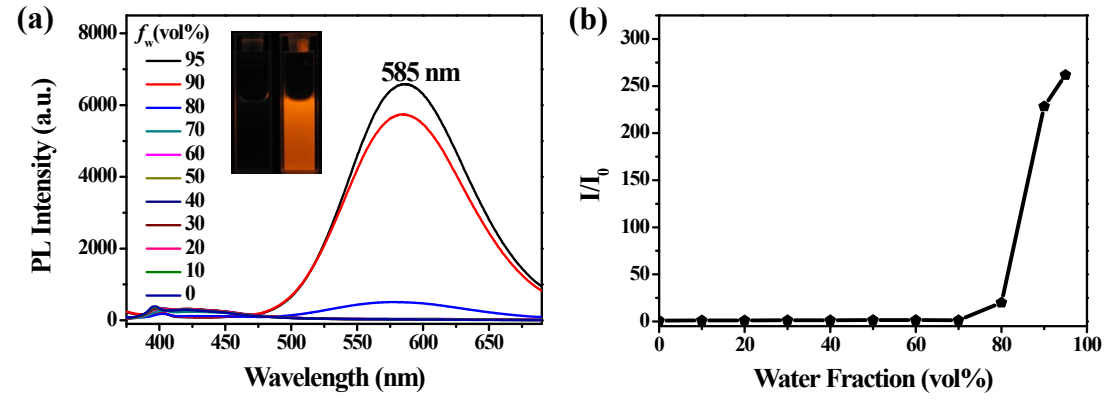

Figure S10. (a) Fluorescence spectra of **TPBD-CN** in THF/water mixtures with different water fractions f_w (concentration: 2×10^{-5} M; excitation wavelength: 355 nm); (b) Plot of relative PL intensity (I/I_0) *vs* f_w. Inset: Photographs of **TPBD-CN** in THF (left) and THF/water mixtures (f_w = 90 vol%, right) under the illumination with 365 nm

UV light.

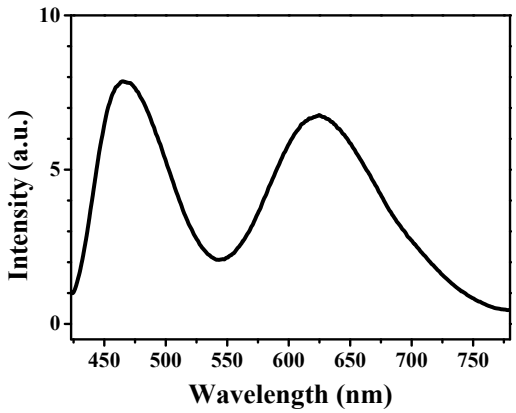

Figure S11. Delayed PL emission spectrum of **TPBD-1** in crystal state (t_d = 0.1 s, excitation wavelength: 400 nm).

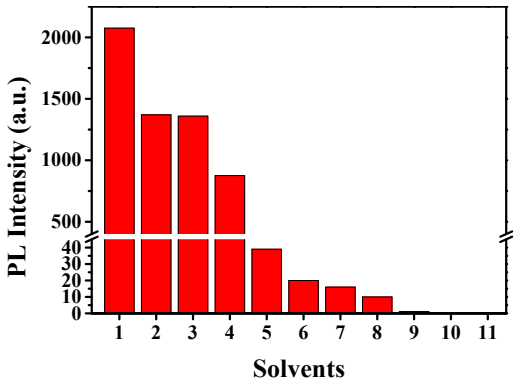

Figure S12. Fluorescence response of **TPBD-1** to TFA in various solvents. Concentration of **TPBD-1** was 2×10^{-5} M; Concentration of TFA was 2×10^{-1} M for entries 1~4 and 2 M for entries 5~11. (1. Chloroform; 2. Dichloromethan; 3. Hexane; 4. Toluene; 5. Diethyl ether; 6. Acetonitrile; 7. Acetone; 8. Methanol; 9. Tetrahydrofuran; 10. Dimethyl sulfoxide;11. Dioxane.)

Table S3. Quantum yield of **TPBD-1** in chloroform before and after the addition of TFA

	Before[a]		After[b]
Sample	Φ_F	λ_{em} (nm)	Φ_F
TPBD-1	<0.01%	660	11.34%

[a]Measured using quinine sulphate in 0.1 M H_2SO_4 as standard (0.54);

[b]Measured using rhodamine B in ethanol as standard (0.69).

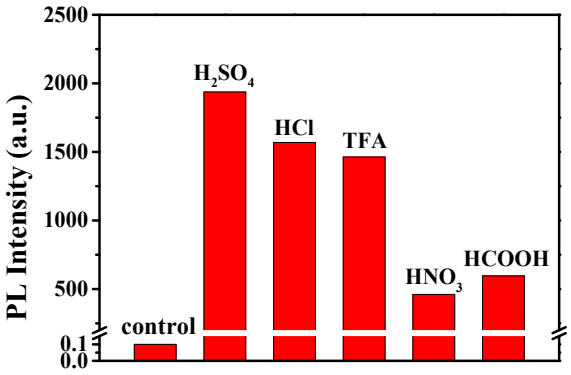

Figure S13. Fluorescence response of **TPBD-1** to various acids in chloroform. Concentration of **TPBD-1** was 1×10^{-4} M; concentration of HCOOH and other acids was 5×10^{-1} M and 5×10^{-2} M, respectively.

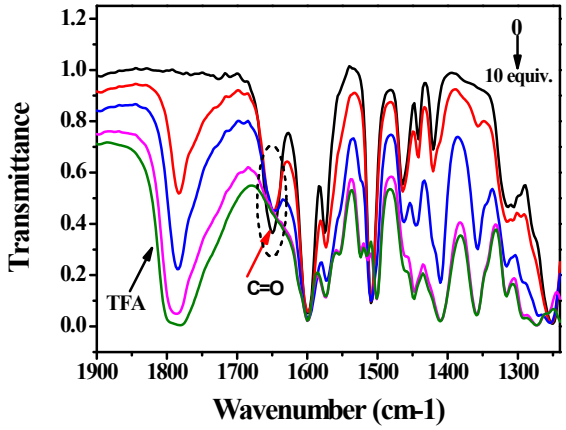

Figure S14. FT-IR spectra of **TPBD-1** in chloroform when treated with TFA (0, 1, 2, 5, 10 equiv.). Concentration of **TPBD-1**: 0.2 mol/L.

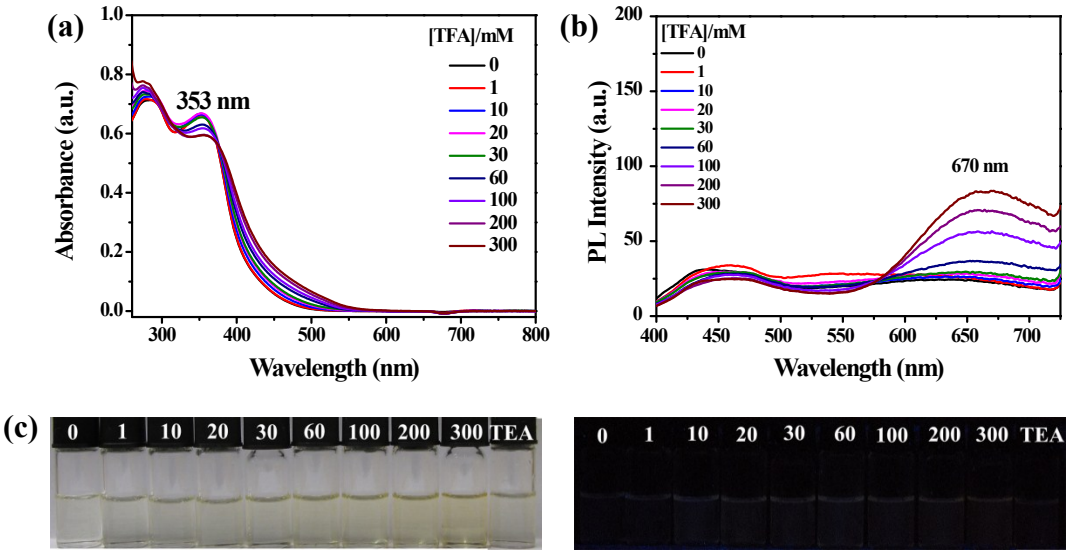

Figure S15. (a) UV-Vis absorption spectra and (b) fluorescence spectra of **TPBD-CN** in chloroform with different concentrations of TFA. (c) Photographs of **TPBD-CN** with the titration of TFA and treatment with TEA in chloroform (taken under natural light and under the illumination with 365 nm UV light). Concentration of **TPBD-CN**: 2×10^{-5} mol/L, excitation wavelength: 357 nm.

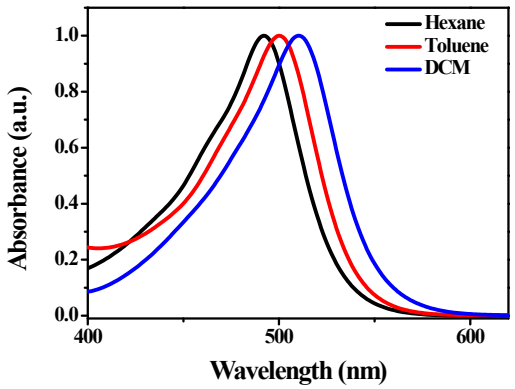

Figure S16. UV-Vis absorption spectra of **TPBD-1** when treated with TFA in different solvents.

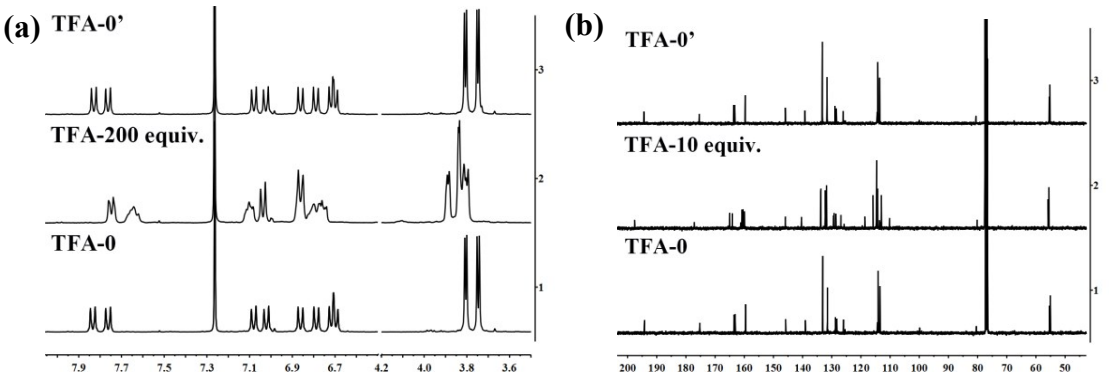

Figure S17. (a) ^{1}H NMR spectra for **TPBD-CN** (5 mM) in $CDCl_3$ after the addition of TFA (200 equiv.). (b) ^{13}C NMR spectra for **TPBD-CN** (50 mM) in $CDCl_3$ after the addition of TFA (10 equiv.). TFA-0': NMR spectra measured after removal of TFA under vacuum.

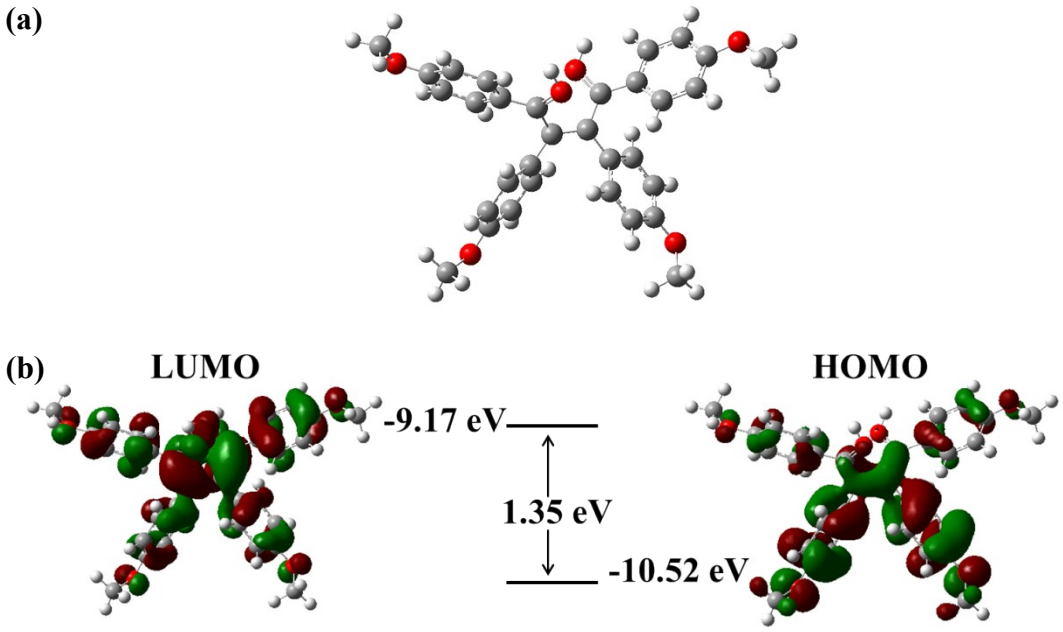

Figure S18. (a) Optimized geometric structure and (b) molecular-orbital amplitude plots and energy levels of the HOMO and LUMO for $[TPBD\text{-}1–2H]^{2+}$ in the gas phase, as calculated at the level of B3LYP/6-31G*.

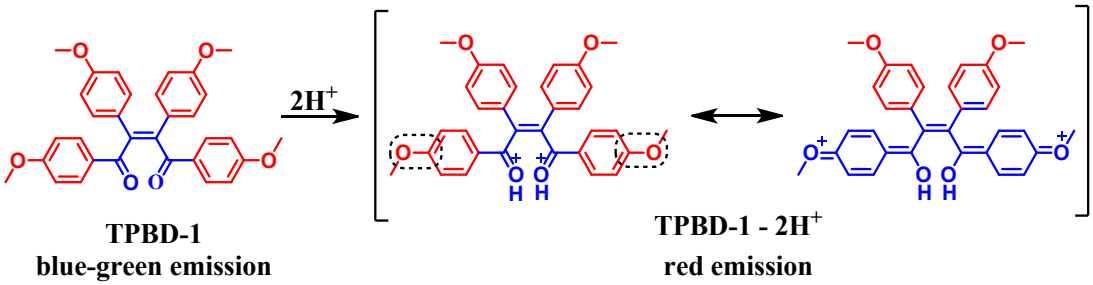

Scheme S2. Proposed mechanism for the formation of **TPBD-1**–TFA complex.

Figure S19. Test of Tyndall effect (left: **TPBD-1** + TFA in chloroform; right: **TPBD-1** in THF/water mixtures with f_w = 95 vol%). Concentration of **TPBD-1**: 2 × 10^{-5} M.

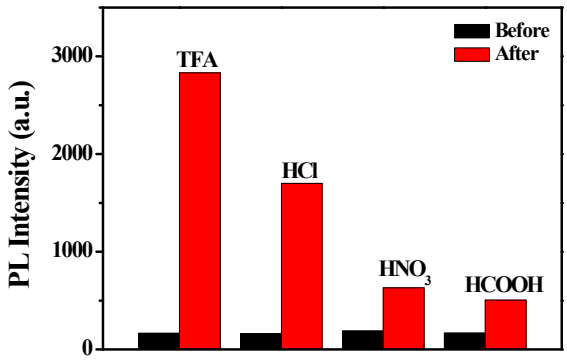

Figure S20. Fluorescence response of **TPBD-1** deposited on a piece of filter paper to the vapors of various acids.

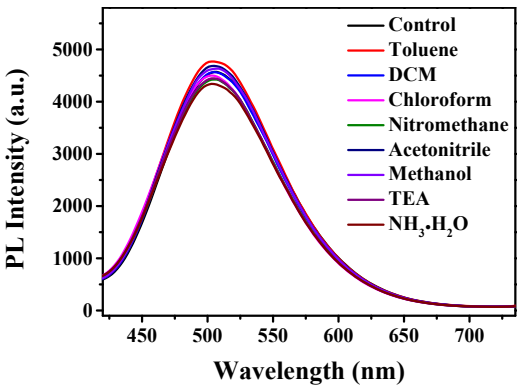

Figure S21. Fluorescence response of **TPBD-1** deposited on a piece of filter paper to

the vapors of netural and basic organic solvents.

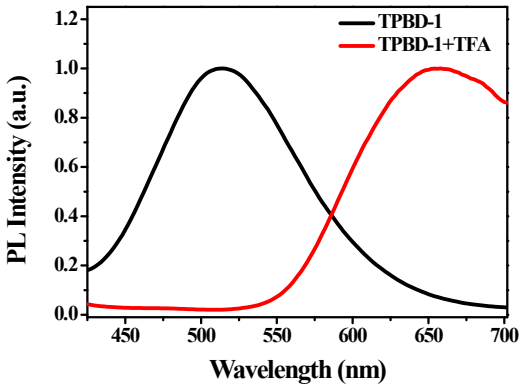

Figure S22. PL spectra of **TPBD-1** deposited on a piece of filter paper before and after fumed with vapor of TFA. Excitation wavelength: 380 nm.

NMR Spectra:

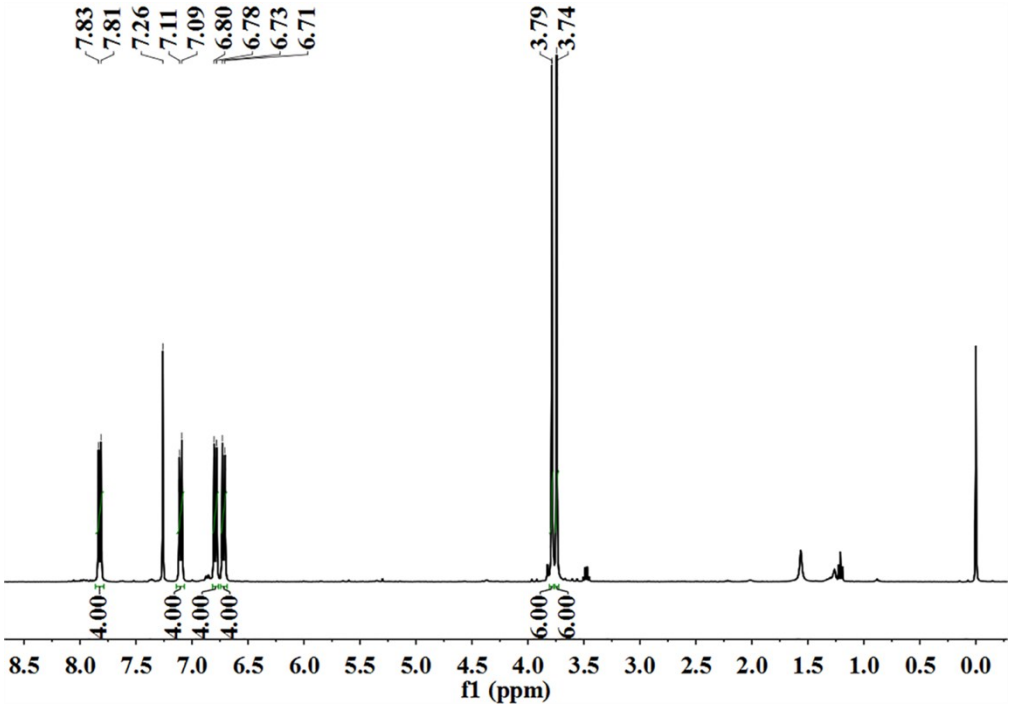

Figure S23. ^{1}H NMR spectrum of (*Z*)-1,2,3,4-tetrakis(4-methoxyphenyl)but-2-ene-1,4-dione **2** in $CDCl_3$.

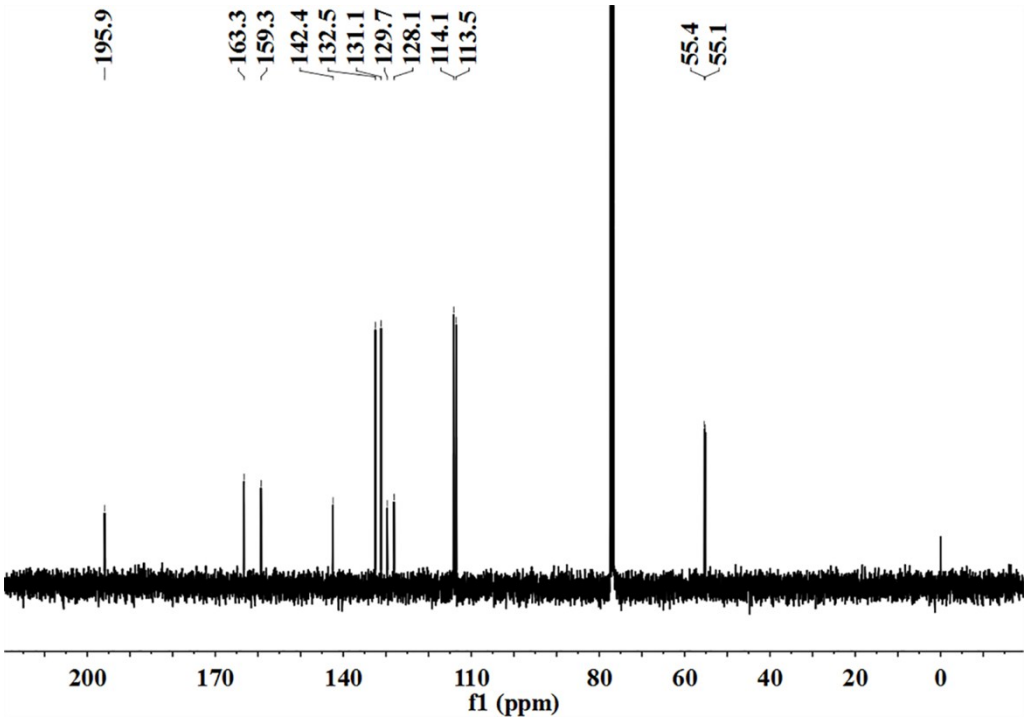

Figure S24. ^{13}C NMR spectrum of (*Z*)-1,2,3,4-tetrakis(4-methoxyphenyl)but-2-ene-1,4-dione **2** in $CDCl_3$.

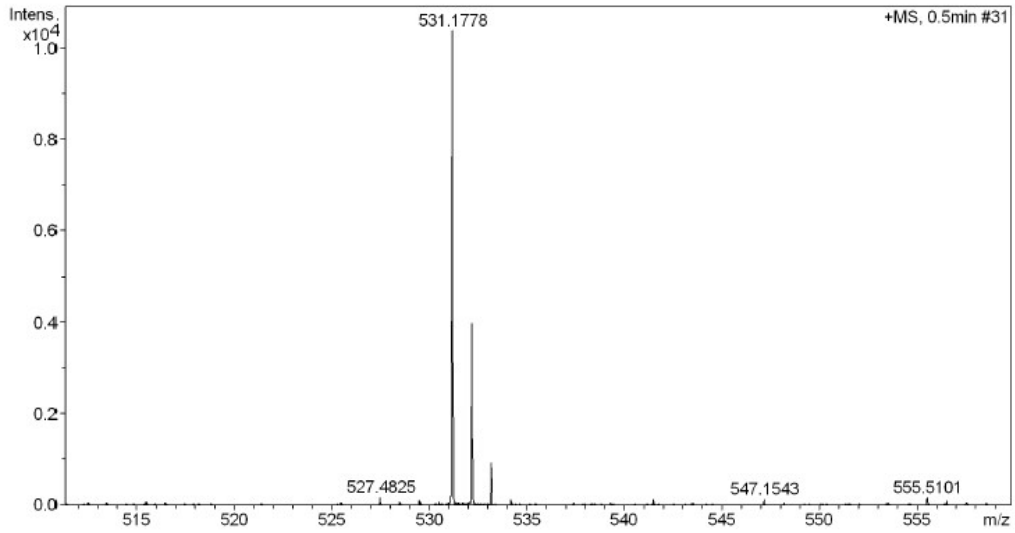

Figure S25. MALDI-TOF spectrum of (*Z*)-1,2,3,4-tetrakis(4-methoxyphenyl)but-2-ene-1,4-dione **2**.

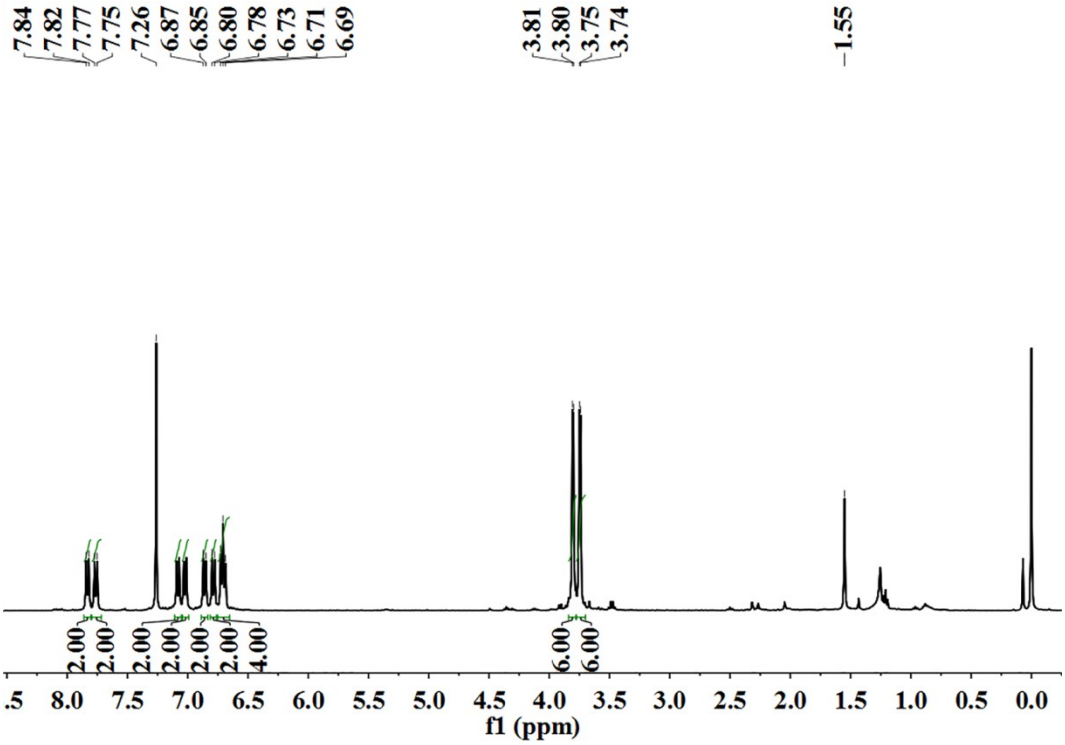

Figure S26. ^{1}H NMR spectrum of (*Z*)-2-(1,2,3,4-tetrakis(4-methoxyphenyl)-4-oxobut-2-en-1-ylidene)malononitrile **3** in $CDCl_3$.

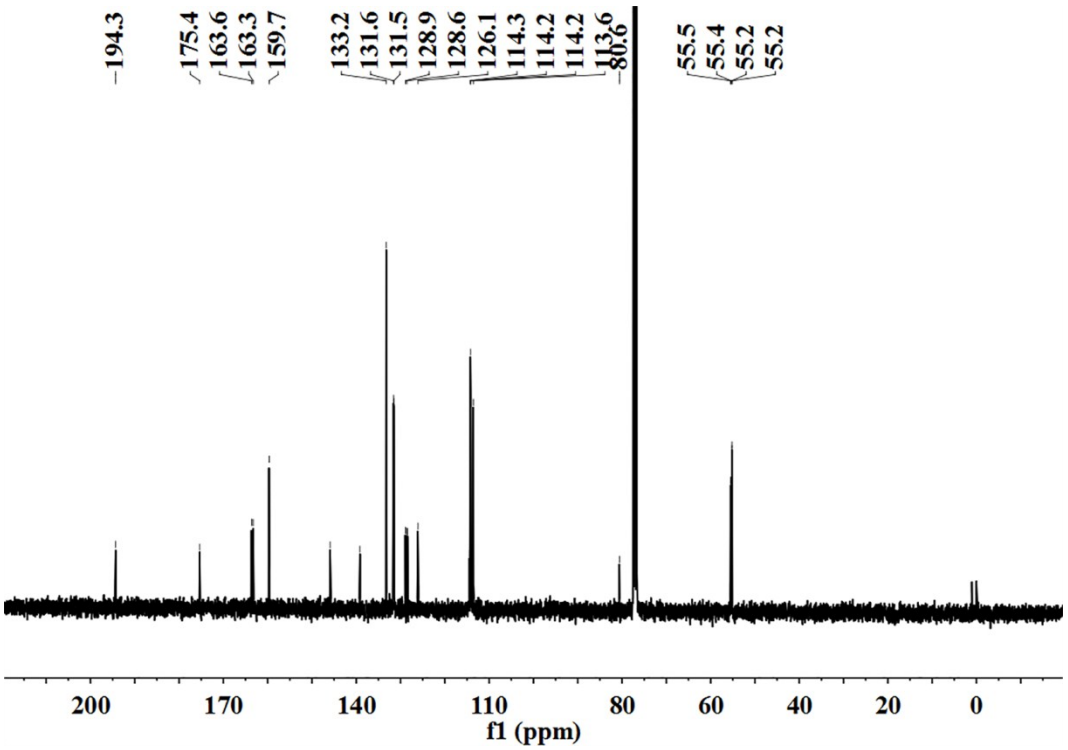

Figure S27. ^{13}C NMR spectrum of (*Z*)-2-(1,2,3,4-tetrakis(4-methoxyphenyl)-4-oxobut-2-en-1-ylidene)malononitrile **3** in $CDCl_3$.

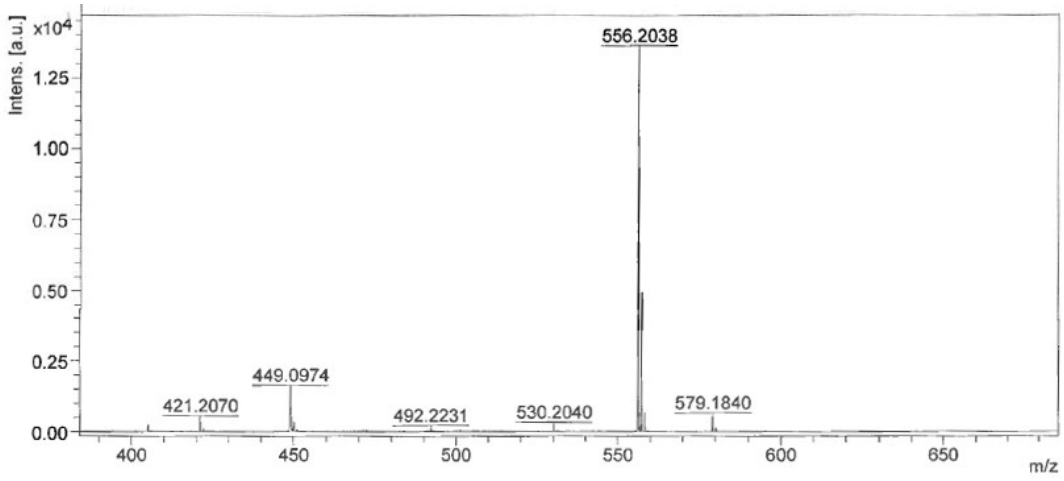

Figure S28. MALDI-TOF spectrum of (*Z*)-2-(1,2,3,4-tetrakis(4-methoxyphenyl)-4-oxobut-2-en-1-ylidene)malononitrile **3**.

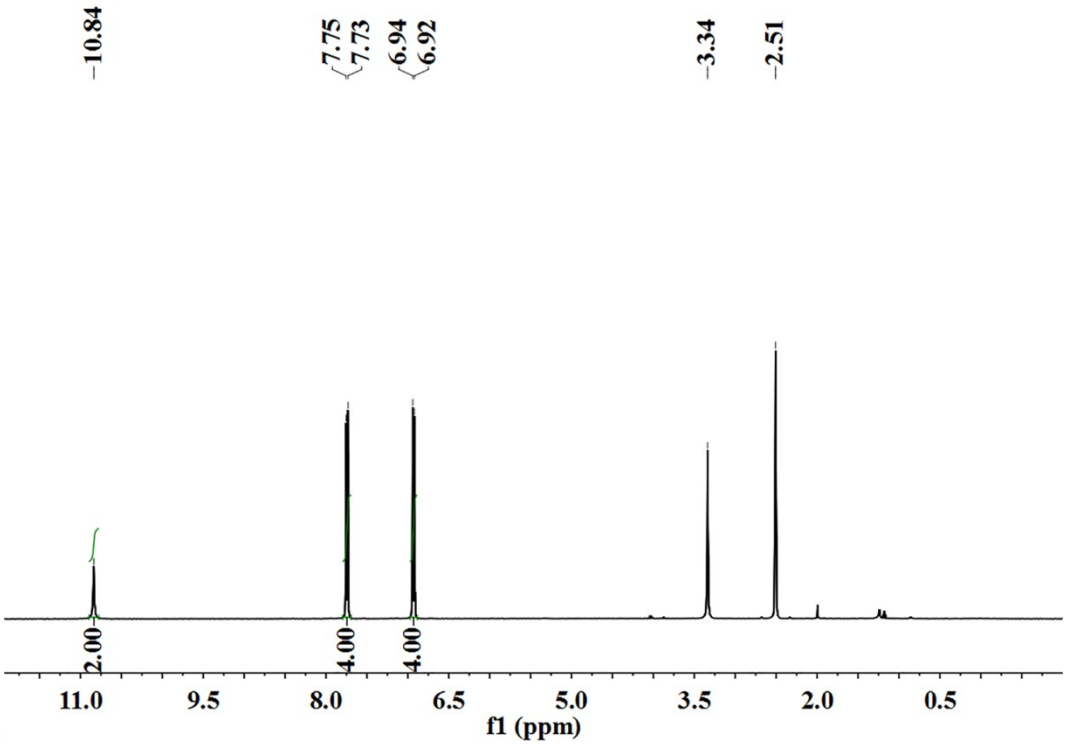

Figure S29. ^{1}H NMR spectrum of 4,4'-dihydroxybenzil **4** in DMSO-d_6.

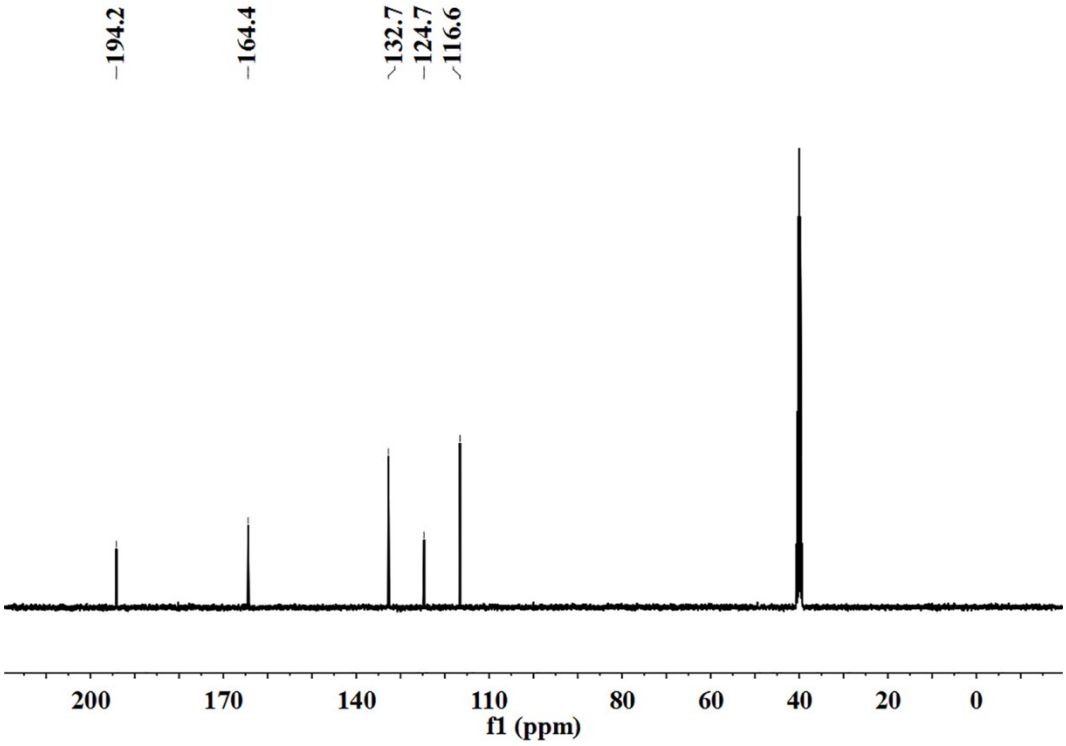

Figure S30. ^{13}C NMR spectrum of 4,4'-dihydroxybenzil **4** in DMSO-d_6.

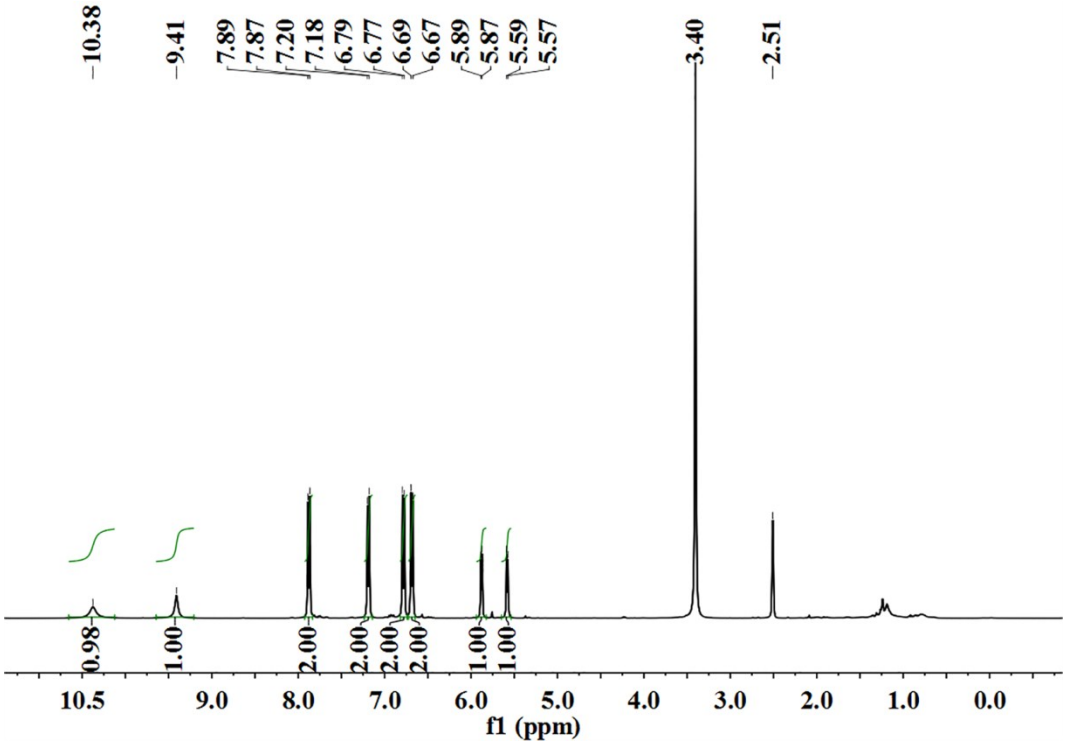

Figure S31. ^{1}H NMR spectrum of 4,4'-dihydroxybenzoin **5** in DMSO-d_6.

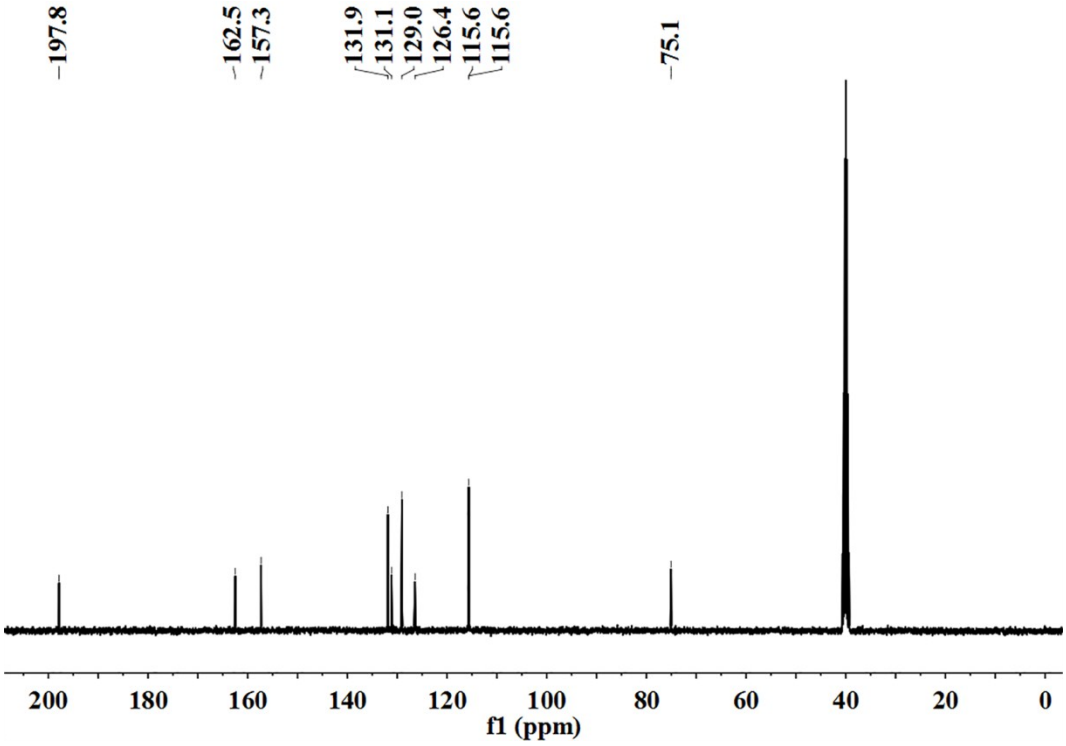

Figure S32. ^{13}C NMR spectrum of 4,4'-dihydroxybenzoin **5** in DMSO-d_6.

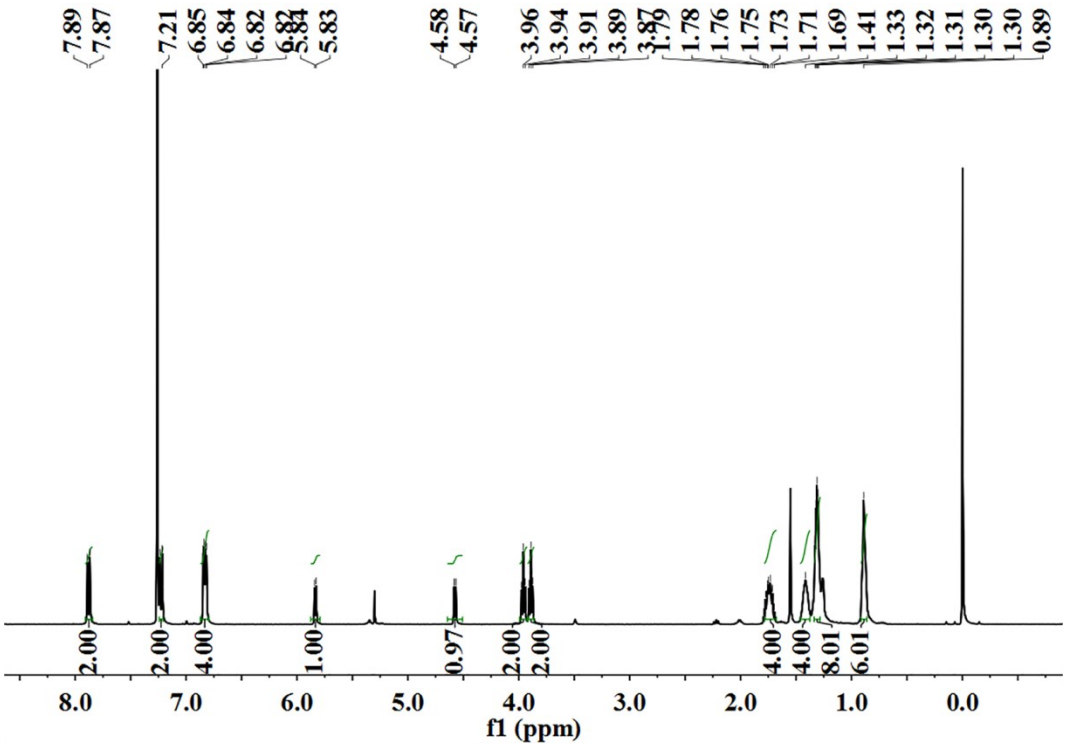

Figure S33. ^{1}H NMR spectrum of 4,4'-dihexyloxybenzoin **6** in $CDCl_3$.

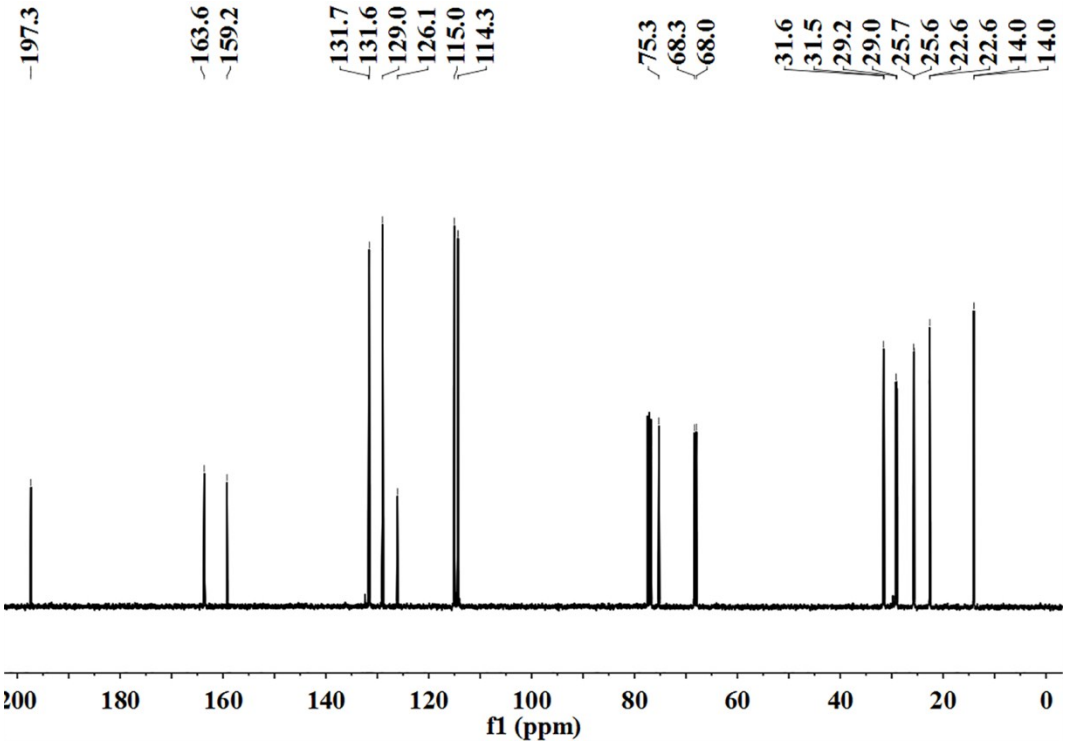

Figure S34. ^{13}C NMR spectrum of 4,4'-dihexyloxybenzoin **6** in $CDCl_3$.

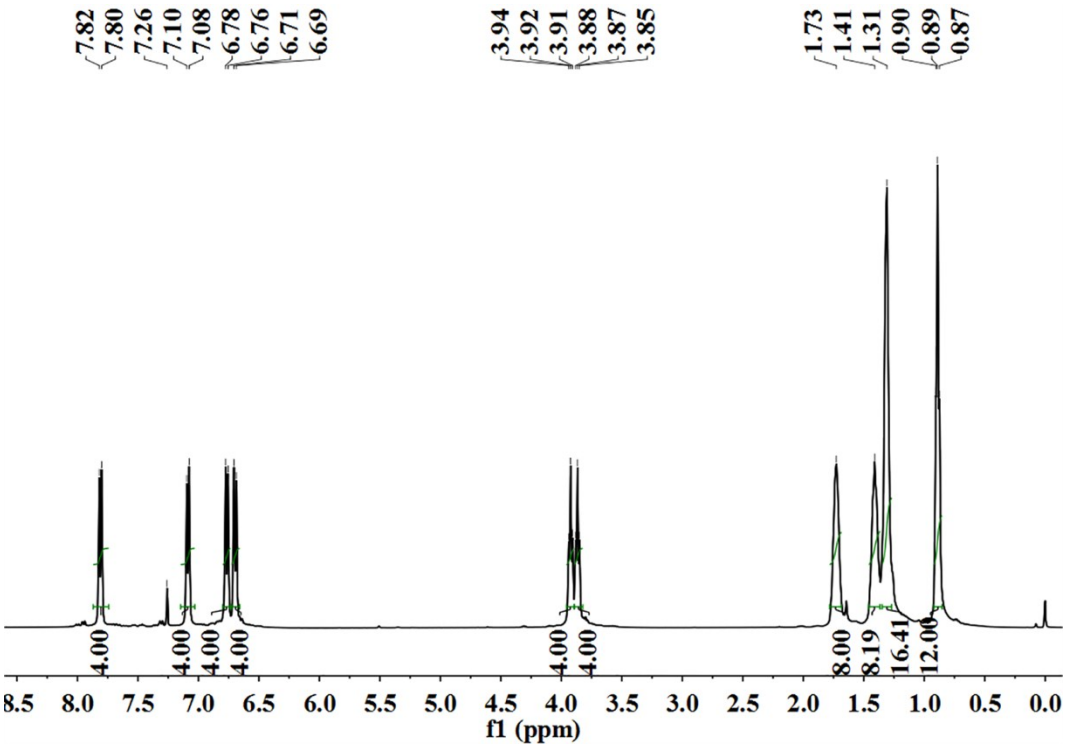

Figure S35. ^{1}H NMR spectrum of (*Z*)-1,2,3,4-tetrakis(4-(hexyloxy)phenyl)but-2-ene-1,4-dione **7** in $CDCl_3$.

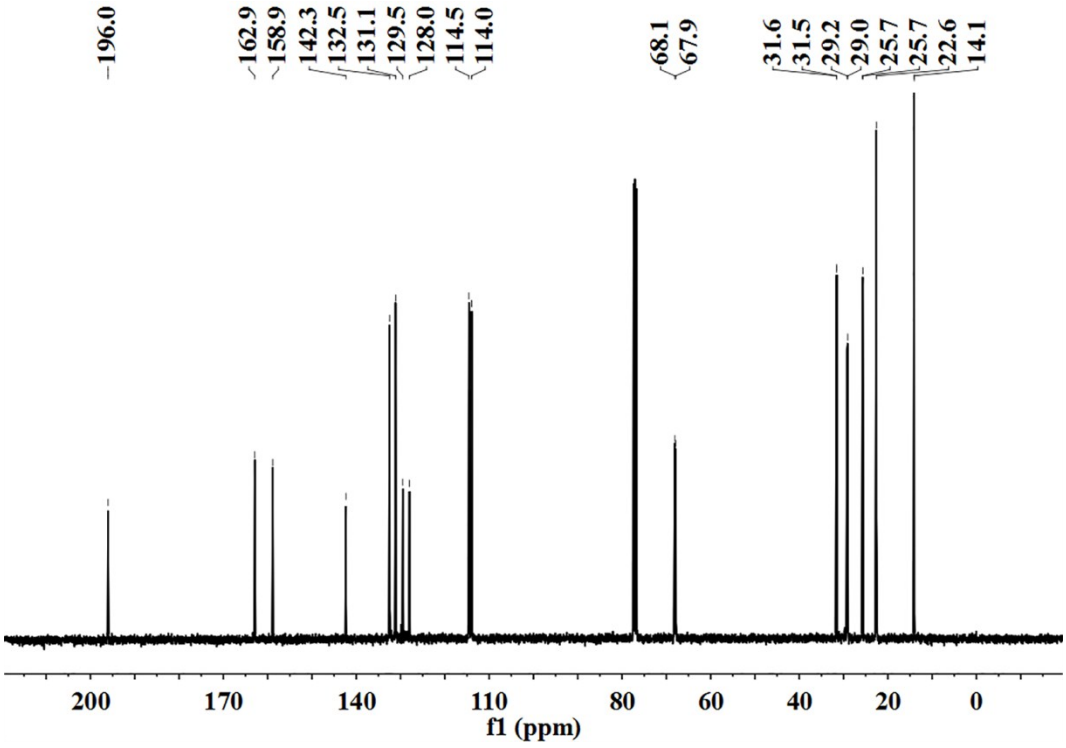

Figure S36. ^{13}C NMR spectrum of (*Z*)-1,2,3,4-tetrakis(4-(hexyloxy)phenyl)but-2-ene-1,4-dione **7** in $CDCl_3$.

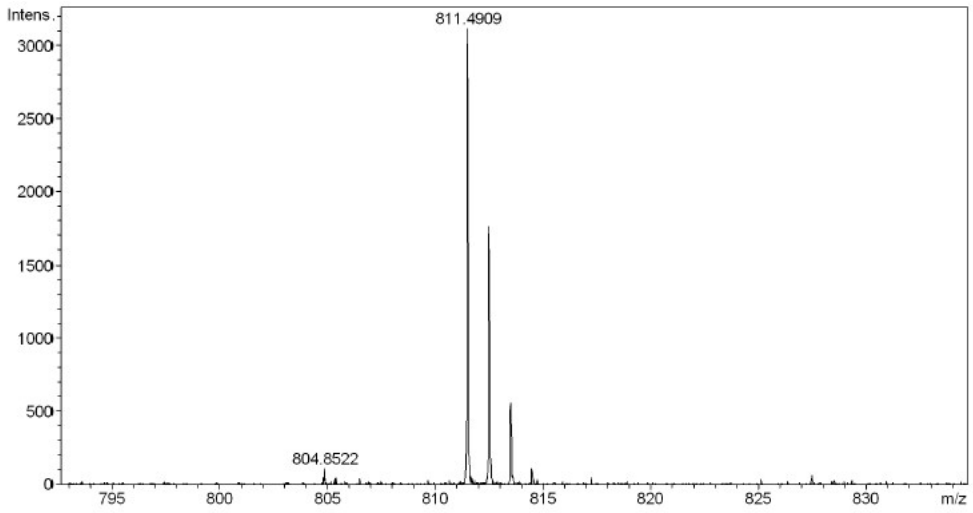

Figure S37. MALDI-TOF spectrum of (*Z*)-1,2,3,4-tetrakis(4-(hexyloxy)phenyl)but-2-ene-1,4-dione **7**.

Table S4. Crystal Data of **TPBD-1** (CCDC: 1523304)

Experical formula	C32H28O6
Space group	P -1
Cell lengths	a/Å 7.5291(15) b/Å 9.914(2) c/Å 17.893(4)
Cell angles	α/° 81.02(3) β/° 83.55(3) γ/° 75.21(3)
Cell volume	1271.84 /Å^3
Z, Z'	Z: 2 Z': 0
R-Factor (%)	3.78

References

S1. R. R. Hu, E. Lager, A. Aguilar-Aguilar, J. Z. Liu, J. W. Y. Lam, H. H. Y. Sung, Ia. D. Williams, Y. C. Zhong, K. S. Wong, E. E. Peña-Cabrera and B. Z. Tang, *J. Phys. Chem. C*, 2009, **113**, 15845.

S2. B. P. Jiang, D. S. Guo and Y. Liu, *J. Org. Chem.*, 2011, **76**, 6101.

S3. R. Shukla, S. H. Wadumethrige, S. V. Lindeman R. Rathore, *Org. Lett.*, 2008, **10**, 3587.